

# Novel Fresnel-zoned microstructured fibre for light waveguiding and efficient coupling between SMF and photonic crystals

Makiko Hisatomi<sup>† ‡</sup>, Michael C. Parker<sup>†</sup>, and Stuart D. Walker<sup>‡</sup>

<sup>†</sup> Fujitsu Laboratories of Europe, <sup>‡</sup> University of Essex

**Abstract:** We describe a low refractive-index contrast (RIC) Fresnel-zoned microstructured fibre (FZ-MSF) for novel waveguiding and low aberration focusing. Due to its confinement mechanism, this microstructured waveguide may find application in nonlinear optics, whilst multiple quarter-period lengths may allow efficient coupling between  $9\ \mu\text{m}$  single-mode fibre (SMF) and  $0.3\ \mu\text{m}$ -dimensioned high refractive-index photonic crystals. We present results of a FZ-MSF design, with a quarter-period of  $4.42\ \mu\text{m}$ , average refractive-index 2.3, and with 0.4 RIC. We estimate it could be used to couple light between SMF and photonic crystals with 0.4dB insertion loss.

## 1 Introduction

Recently, microstructured fibres (MSFs), such as Bragg fibre [1,2] and photonic crystal fibres (PCFs) [3], have been the focus of increasing scientific and technological interest. Photonic crystals (PhCs) with high refractive index contrast (RIC) have also attracted much interest lately [4], as an underlying technology for photonic integrated circuits (PICs). However, due to the high index difference between  $\text{SiO}_2$  and semiconductor devices, coupling between single-mode fibre (SMF) and PhC remains a significant challenge for PICs based on PhCs. Typical PhC waveguide dimensions for single-mode transmission are  $0.3\ \mu\text{m} \times 0.3\ \mu\text{m}$ , whereas the spot size diameter of SMF is approximately  $9\ \mu\text{m}$ . Various approaches to achieve low-loss coupling between SMF and PhC have been made, such as spot-size conversion [5], and a butt-jointable PhC waveguide [6]. In this paper, we describe a method to efficiently couple light between SMF and PhC using a novel Fresnel-zoned (FZ) MSF waveguide lens. Figure 1(a) shows a schematic diagram of the proposed FZ-MSF waveguide. FZ's are well understood and have been extensively investigated, but have tended to be applied in a free-space configuration. Recently, workers at Sydney University have fabricated holey MSF incorporating holes distributed with radius varying in the well-known parabolic fashion of Fresnel zone plates [7]. However our FZ-MSF guides light in a similar way to a graded-index (GRIN) fibre, but employs refractive index discontinuities at the FZ boundaries in order to keep the refractive index contrast low. Superficially, our FZ-MSF design looks similar to Bragg fibre [1,2] which consists of concentric rings of different refractive indices such that the incremental radius of each ring is equivalent to a constant  $\lambda/4$  path length change. Light at the Bragg wavelength is reflected back into the core by the photonic bandgap effect, and hence is guided. However, due to the graded-index variation, our FZ-MSF fibre periodically focuses light back into the centre in order to achieve waveguiding. Instead of having a continuous parabolic refractive index variation of standard GRIN fibre, our MSF employs longitudinal FZs to focus the light within the actual fibre structure. Since a quarter-period of the FZ-MSF is analogous to a focal length, our structure can therefore also be used to focus light from SMF down to PhC dimensions, and vice-versa.

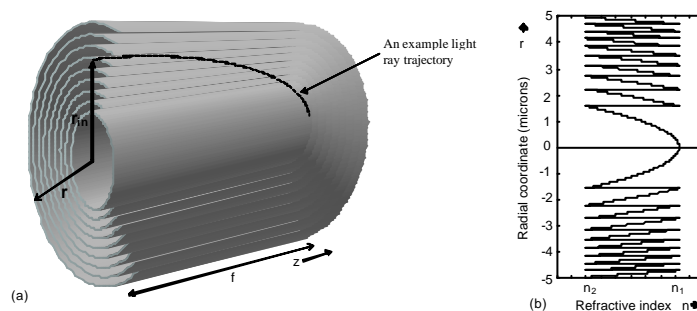


Fig.1: (a) Schematic diagram of FZ-MSF waveguide lens, (b) refractive index profile  $n(r)$  for FZ-MSF waveguide

## 2. Theory

We have employed the principle of least time (Fermat's principle) to analyse the propagation of light in our waveguiding structure. This has the advantage of reduced computational effort, as compared with a beam propagation modal analysis, but also yields a deeper insight into the waveguiding properties and aberration (dispersive) characteristics of our device.

## 2.1 Equation of light trajectory

The equation describing the trajectory of a light ray in a medium with a spatially varying refractive index is [8]:

$$\frac{d}{dt} \left( n(\underline{x}) \frac{d\underline{x}}{dt} \right) = \nabla n(\underline{x}), \quad (1)$$

where  $n(\underline{x})$  is the refractive index distribution as a function of space  $\underline{x}$ , and  $t$  is the (scalar) trajectory of the ray. Using the paraxial approximation, and assuming only radial variation in refractive index, equation (1) can be simplified to a second-order differential equation, as a function of longitudinal co-ordinate  $z$ , and radial co-ordinate  $r$ :

$$\frac{d^2 r}{dz^2} = \frac{1}{n(r)} \frac{dn}{dr}. \quad (2)$$

## 2.2 Gaussian GRIN refractive index profile

It is straight forward to show that substitution into equation (2) of a Gaussian GRIN refractive index profile  $n(r) = n_1 \exp(-\mathbf{k}_1^2 r^2 / 2)$  leads to the simple-harmonic motion equation  $d^2 r / dz^2 = -\mathbf{k}_1^2 r$ , which describes a sinusoidal trajectory,  $r = r_{in} \cos \mathbf{k}_1 z + (r'_{in} / \mathbf{k}_1) \sin \mathbf{k}_1 z$ , where  $r_{in}$  is the input radius of the trajectory,  $r'_{in}$  is the initial slope of the trajectory (prime in this case indicates differentiation w.r.t.  $z$ ), and  $\mathbf{k}_1$  is the parameter for the Gaussian refractive index profile, which therefore also determines the quarter period focal length  $f$  of the GRIN lens, such that  $f = \pi / 2\mathbf{k}_1$ . Hence a Gaussian refractive index profile in a GRIN fibre gives aberration-free (dispersion-less) trajectories, clearly shown in Figure 2, but would be exceedingly difficult to fabricate. Here the fibre parameters are  $n_1 = 3.5$ , maximum core radius is  $a = 5 \text{ mm}$ , and  $\mathbf{k}_1 = 0.3166 \text{ mm}^{-1}$ . The spot-size radius of light focussed from SMF is estimated to be  $w_0 = 0.12 \text{ mm}$ , thus making it suitable for efficient spatial mode coupling between SMF and PhC. However, its very large refractive index variation would cause high reflections at the interfaces, and reduce coupling efficiency.

## 2.3 Elliptical GRIN refractive index profile

A Gaussian refractive index profile can be expanded into a power series, as follows:

$$n(r) = n_1 \exp\left(-\frac{\mathbf{k}_1^2 r^2}{2}\right) \approx n_1 \sqrt{1 - \mathbf{k}_1^2 r^2 + \frac{(\mathbf{k}_1^2 r^2)^2}{2!} - \dots} \quad (3)$$

First order truncation of (3) yields the well-known elliptical refractive index distribution for GRIN fibre:

$$n(r) = n_1 \sqrt{1 - 2\Delta r^2 / a^2} \quad (4)$$

where we can therefore assume that  $\mathbf{k}_1^2 \equiv 2\Delta / a^2$ . The other parameters are given by  $\Delta = (n_1^2 - n_2^2) / 2n_1^2$ , with  $n_1$  being the refractive index at the centre, and  $n_2$  the refractive index at the maximum core radius  $a$ . Substitution of equation (4) into equation (2) yields:

$$\frac{d^2 r}{dz^2} = -\frac{2\Delta}{a^2 - 2\Delta r^2} r \quad (5)$$

If the RIC isn't too high, such that  $2\Delta r^2 \ll a^2$ , equation (5) can be analytically solved to again yield a sinusoidal trajectory,  $r = r_{in} \cos \mathbf{k} z + (r'_{in} / \mathbf{k}) \sin \mathbf{k} z$ , where  $\mathbf{k} \approx \sqrt{2\Delta / a^2}$ . Figure 3 plots the numerical light trajectory solutions to equation (5). Compared with Figure 2 aberration is now evident due to the imperfect focusing of the light rays. For comparison with the Gaussian case, figure 3 shows the ray trajectories for the closest equivalent elliptical GRIN fibre with continuous refractive index variation,  $n_1 = 3.5$ ,  $n_2 = 1$ , and maximum core radius  $a = 5 \text{ mm}$ . In this case, the equivalent spatial frequency is  $\mathbf{k} = 0.1917 \text{ mm}^{-1}$ , yielding a longer theoretical quarter-period (focal length) of  $f \sim 8 \text{ mm}$ . Such a fibre (which again would be difficult to fabricate) can only produce a spot size of  $w_0 = 0.22 \text{ mm}$ , leading to less-efficient coupling of light between SMF

and PhC. In addition, similar to the Gaussian case, its very large refractive index variation would cause high reflections at the interfaces.

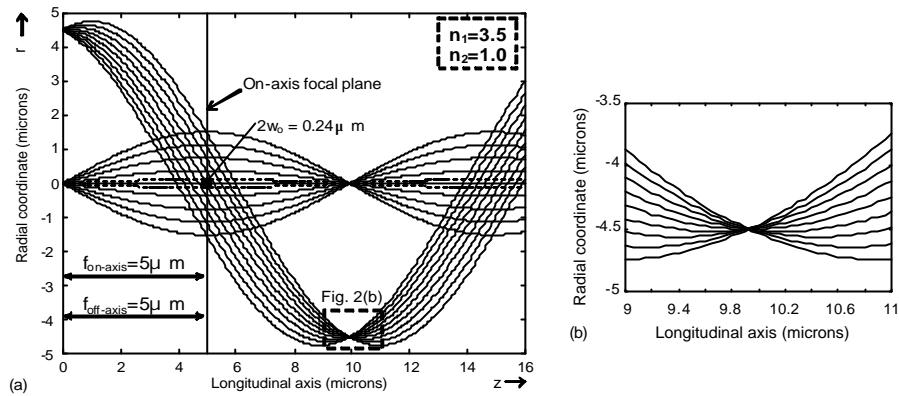


Figure 2: (a) Ray trajectories for Gaussian GRIN fibre, (b) zoomed in diagram for Gaussian GRIN fibre.

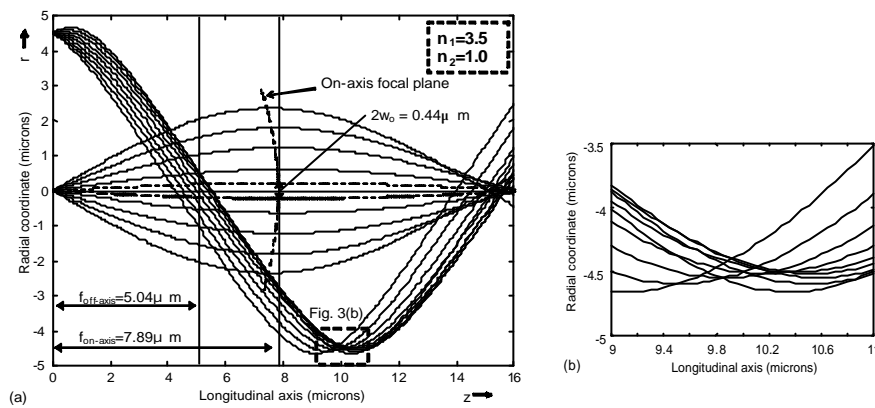


Figure 3: (a) Ray trajectories for elliptical GRIN fibre, (b) zoomed in diagram for elliptical GRIN fibre

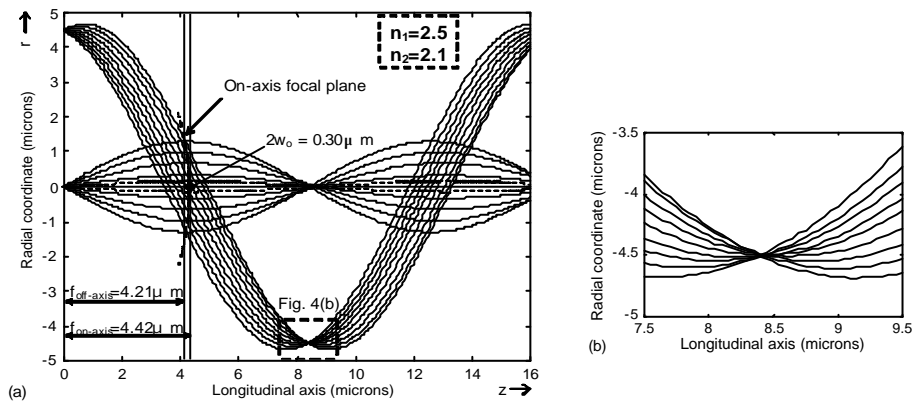


Figure 4: (a) Ray trajectories for parabolic FZ-MSF, (b) zoomed in diagram for parabolic FZ-MSF

## 2.4 Fresnel-zoned parabolic refractive index profile

In order to reduce reflections at the PhC, FZ-MSF, and SMF interfaces, the RIC must be reduced. This allows us to further approximate equation (4) using a binomial expansion for the square root, assuming the refractive index contrast  $\Delta n$  is low, to yield a parabolic expression for the refractive index profile:

$$n(r) = n_1 \left( 1 - \Delta r^2 / a^2 \right). \quad (6)$$

However, this now allows us to adopt a Fresnel-zone strategy to keep the refractive index contrast low. This is possible because equation (6) is a parabola conforming to the well-known paraxial approximation for thin lenses,

in which case the radius of the  $m^{\text{th}}$  zone is given by  $r_m = \sqrt{m}r_1$ . The resulting refractive index variation  $n_m(r)$  for the  $m^{\text{th}}$  FZ, equivalent to the continuous profile of equation (6), is given by:

$$n_m(r) = n_1 - \frac{(n_1 - n'_m(r))(n_1 - n_2)N}{n_1\Delta} \quad (7a)$$

$$n'_m(r) = n_1 \left(1 - \Delta r^2 / a^2\right) + \frac{(m-1)n_1\Delta}{N} \quad (7b)$$

Figure 1(b) shows the refractive index profile of the proposed FZ-MSF lens, with a maximum radius of  $a = r_N = 5\text{mm}$ , consisting of  $N=10$  zones, with  $n_1 = 2.5$ ,  $n_2 = 2.1$ . The light trajectories for this FZ-MSF are shown in Figure 4.

### 3. Discussion

Figures 2-4 show on-axis and off-axis ray trajectories up to the maximum numerical aperture (NA) of the FZ-MSF for the Gaussian, elliptical and FZ-MSF (discontinuous parabolic) RI profiles respectively. The NA associated with SMF is much smaller, and the corresponding on-axis trajectory for this is shown as a dotted line. The dotted line in Figure 4(a) indicates that the FZ-MSF produces a spot-size of  $2w_0=0.30\text{mm}$  for the SMF NA, making it appropriate for efficient spatial mode-matching with the PhC. The average FZ-MSF refractive index of 2.3 is close to the theoretical power-matching refractive index  $\sqrt{n_{SMF}n_{PhC}} = 2.29$  for minimum reflection between SMF ( $n_{SMF}=1.5$ ), FZ-MSF, and PhC (e.g. silicon,  $n_{PhC}=3.5$ ) leading to a reduced reflection loss of 0.2dB at each of the two interfaces, as compared with the Gaussian and elliptical cases. Apparent from Figures 2(a), 3(a) and 4(a) is that the Gaussian profile provides the ideal trajectories, whilst tighter and more symmetrical focussing is achieved for the FZ-MSF as compared with the elliptical profile, leading to superior spatial-mode preservation and more efficient coupling into PhC. The lower aberration of the FZ-MSF (focal lengths varying only between 4.21 and 4.42 mm for the on- and off-axis cases respectively, compared with 5.04 and 7.89 mm for the elliptical fibre) is attributed to the smaller absolute radial variation in refractive index. Since the FZ-MSF has refractive variation between only 2.1 and 2.5, this is much closer to the ideal than for the elliptical fibre with index variation between 1 and 3.5. This also indicates that a greater number of Fresnel zones  $N$  (allowing a still lower refractive index difference) leads to closer ideal lens behaviour.

### 4. Conclusions

We have presented a novel Fresnel-zoned MSF waveguide design with a discontinuous parabolic refractive index profile, featuring low  $\Delta n=0.4$  refractive index contrast, for efficient light coupling between SMF and PhCs. Further work is concerned with the geometry of a binary refractive index case, which whilst offering sub-optimal performance, may provide fabrication advantages.

### References

- [1] P.Yeh, A.Yariv and E.Marom, "Theory of Bragg fibre", J. Opt.Soc.Am., Vol.68, No.9, September 1978
- [2] M.Ibanescu, S.G.Johnson, M.Soljacic, J.D.Joannopoulos, Y.Fink, O.Weisberg, T.D.Engeness, S.A.Jacobs and M.Skorobogatiy, "Analysis of mode structure in hollow dielectric waveguide fibers", Phys.Rev. E, Vol.67(4), article No. 046608, 2003
- [3] J.C.Knight, T.A.Birks, P.St.J.Russell and D.M.Atkin, "All-silica single mode fibre with photonic crystal cladding", Opt.Lett. 21 (1547-1549) 1996
- [4] J. D. Joannopoulos, R.D. Meade, J.N. Winn, "Photonic Crystals", Princeton University Press, 1995
- [5] T.Shoji, T.Tsuchizawa, T.Watanabe, K.Yamada and H.Morita, "Spot-size converter for low-loss coupling between  $0.3\mu\text{m}^2$  Si wire waveguides and single-mode fibres", 15<sup>th</sup> LEOS conference proceedings, Vol.1, TuU3, pp289-290, 2002
- [6] T.Saito, Y.Ohtera, T.Kawashima, H.Ohkubo, K.Miura, N.Ishino, S.Kawakami, "Fibre Butt-jointable Waveguide and Wavelength Filter Consisting of Photonic Crystals", 28<sup>th</sup> ECOC conference proceedings, Vol.2, 4.4.2, 2002
- [7] J.Canning, E.Buckley, K.Lyytikainen, "Propagation in air by field superposition of scattered light within a Fresnel fibre", Opt.Lett. Vol.28, No.4, Feb.15, 2003
- [8] M.Born, E.Wolf, "Principles of Optics", Chapter 3, Pergamon Press, 6<sup>th</sup> ed., 1984